JOURNAL OF PHYSICAL ORGANIC CHEMISTRY
J. Phys. Org. Chem. 2005; **18:** 417–425
Published online 15 December 2004 in Wiley InterScience (www.interscience.wiley.com). DOI: 10.1002/poc.889

Density functional theory study of palladium-catalyzed aryl-nitrogen and aryl-oxygen bond formation

Thomas R. Cundari* and Jun Deng

Department of Chemistry, University of North Texas, Denton, TX 76203-5070, USA

Received 28 August 2004; revised 18 October 2004; accepted 18 October 2004

ABSTRACT: A density functional theory study of the kinetics and thermodynamics of Pd-phosphine-catalyzed heteroatom bond formation

$$ArX + REH_n \xrightarrow[[Pd]]{} ArE(H)_{n-1}R + HX$$

was carried out. Individual steps in the catalytic cycle—ArX oxidative addition, REH_n coordination, HX loss and $ArE(H)_{n-1}R$ reductive elimination and β-hydride elimination—were investigated. The effects of modification of the ligand (PH_3 versus PMe_3), leaving group (X = Cl versus X = Br), heteroatom substrate ($REH_n = H_2O$ and NH_3), aryl (Ar = phenyl, *p*-cyanophenyl, *p*-aminophenyl, pyridyl) and metal coordination number ($Pd(PH_3)$ versus $Pd(PH_3)_2$) were investigated. Copyright © 2004 John Wiley & Sons, Ltd.
Supplementary electronic material for this paper is available in Wiley Interscience at http://www.interscience.wiley.com/jpages/0894-3230/suppmat/

KEYWORDS: amination; palladium; density functional theory; effective core potential; organic synthesis

INTRODUCTION

Transition metals are pivotal in catalyzing the reactions by which drugs and drug candidates are synthesized.[1] In the pantheon of catalysts for organic synthesis, palladium (Pd) occupies a pre-eminent spot among transition metals. In addition to its extensive use for the reduction of unsaturated moieties, Pd compounds play a pivotal role in carbon-element bond formation, particularly for systems with allyl, vinyl and aryl entities. Among bond formation reactions catalyzed by palladium complexes, the Trost–Tsuji,[2] Heck,[3] Stille,[4] Suzuki,[5] Buchwald–Hartwig syntheses[6,7] and their derivatives are among the most commonly employed for the synthesis of drugs, drug candidates and bioactive natural products.

Classical methods of aryl-heteroatom bond formation involving electrophilic aromatic substitution or Ullmann–Goldberg-type coupling procedures[8] are typically neither reliable nor efficient, and the harsh conditions required are usually incompatible with pharmaceutical intermediates. Hence, there has been considerable experimental research in the past decade (*vide infra*) to identify transition metal catalysts for carbon-heteroatom bond formation that work with a variety of substrates (organic halides and triflates, arene and heterocyclic species, amines and alcohols, etc.).[6,7] From these efforts, palladium (Pd) complexes, particularly those with phosphine coligands, have emerged as the most promising catalysts in aryl-heteroatom bond formation reactions.

The present computational research is inspired by the experimental work of the Buchwald group (Eqn (1)):

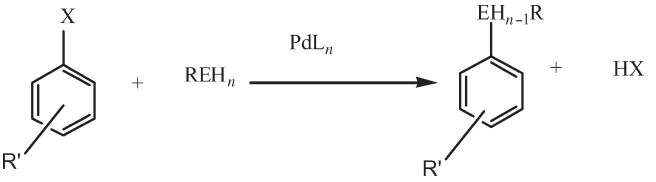

(1)

The phosphines (L_n in Eqn (1)) investigated by Buchwald and co-workers have the form $PR_2(Ar–Ar')$ (Fig. 1), where R is typically a bulky alkyl group such as cyclohexyl (Cy) or *t*-butyl (^{t}Bu) and Ar–Ar′ is a biphenyl derivative.[9]

The activity and selectivity of the Pd–phosphine catalysts for the reaction in Eqn (1) have been found to be sensitive to the steric and electronic profile of the phosphine (e.g. aryl versus alkyl phosphine substituents), the X leaving group of the aryl substrate (chloride versus bromide versus triflate), the E-bearing substrate (alcohols versus amines), whether bond formation is inter- or intramolecular, and even reaction parameters such as solvent and temperature.[6,7]

Despite the massive experimental effort,[1,6,7] Pd-catalyzed aryl-heteroatom bond formation has, to our knowledge, not received attention from theoreticians. Even for amination, the most well-studied reaction,[6,7] there are

**Correspondence to:* T. R. Cundari, Department of Chemistry, University of North Texas, Denton, TX 76203-5070, USA.
E-mail: tomc@unt.edu
Contract/grant sponsor: National Science Foundation; *Contract/grant number:* CHE-9983665.

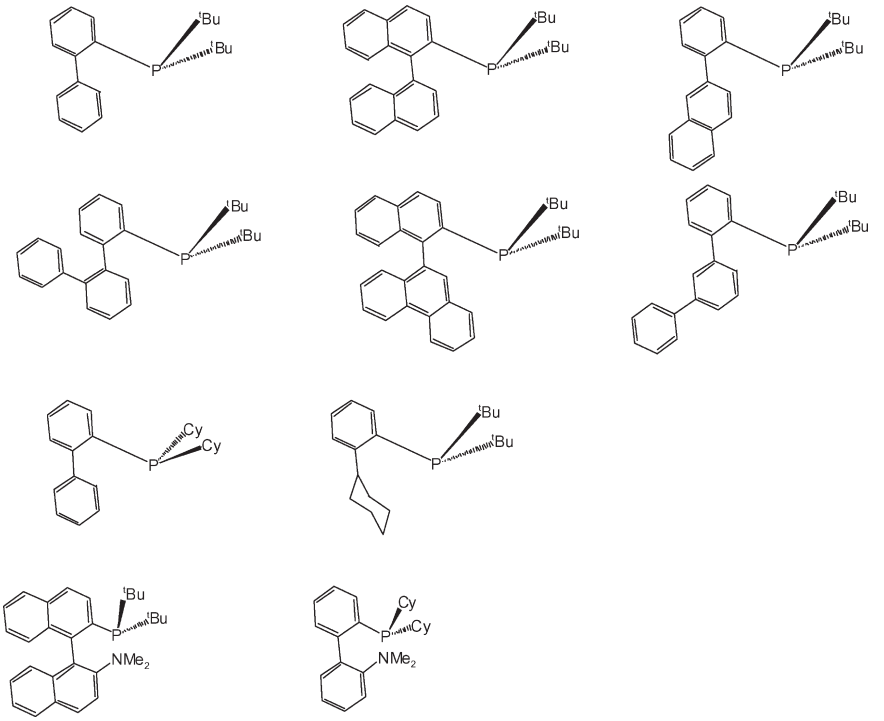

Figure 1. Phosphine co-ligands for palladium-catalyzed carbon-heteroatom bond formation

few quantitative kinetic and thermodynamic data. Surprisingly, there has been little computational study of many important Pd-catalyzed organic transformations. Morokuma and co-workers have investigated some reactions pertinent to Suzuki coupling.[10] Rösch and co-workers have studied some of the proposed mechanisms of the Heck reaction involving Pd-heterocyclic carbene catalysts.[11] Perhaps the most comprehensive theoretical research on a Pd-catalyzed organic synthetic transformation is that reported by Norrby *et al.* on Pd-catalyzed allylic alkylation.[12] This research is an excellent demonstration of the potential for computational chemistry to provide better understanding of transition metal catalyzed organic synthetic transformations, and for the integration of theory and experiment in designed improved catalysts.

Another major unresolved issue in experiment is the exact nature of the catalyst active species. Kocovsky *et al.*[13] have provided NMR evidence for so-called MAP ligands for a dynamic equilibrium involving multiple coordination isomers. This work involved Pd^{II} species, and thus it is unclear if such a situation exists for the catalytically active Pd^0 species in aryl-heteroatom bond formation. Experimental data support a Pd(P∼P) intermediate for bidentate phosphines (P∼P = bis (diphenylphosphino)ferrocene or BINAP).[7] For monodentate phosphines, such as the new biaryl-phosphines (see Fig. 1) reported by Buchwald and co-workers,[14] it is unclear if the active species is a mono- or diphosphine, or whether both pathways are operant.

The paper is written based on the proposed catalytic cycle in Fig. 2. The catalytic cycle involves oxidative addition, heteroatom substrate coordination, HX elimination and reductive elimination (see Results). The β-hydride elimination reaction is the major pathway to unwanted reduced arene side-products and the exact

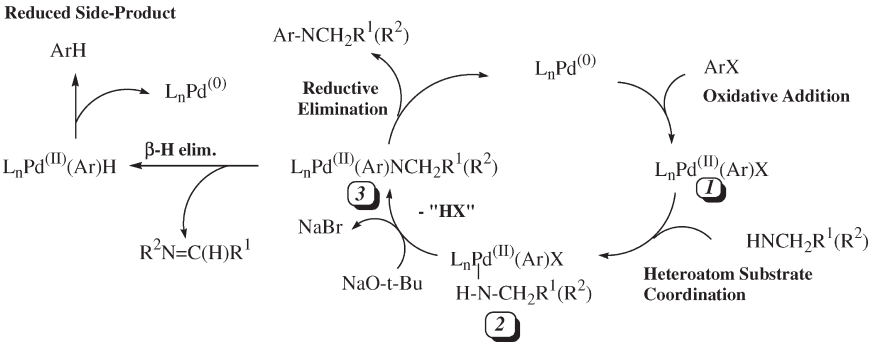

Figure 2. Catalytic cycle for amination. The proposed steps (in bold) are based on current experimental information.[6,7] An analogous catalytic cycle can be drawn for the etheration reaction

nature of the catalyst active species is explored in the Result section.

Calculations aim to provide insight into portions of the proposed catalytic cycle (Fig. 2) for which direct experimental evidence is limited, e.g. the bonding and structure of the putative Pd–phosphine catalyst, the nature of the various transition states, the kinetic partitioning between reductive elimination to form the desired product and β-hydride transfer to yield unwanted, reduced side-products, etc. Following these investigations are computational studies of experimental results concerning the response of the Pd catalysts to modification of the substrate leaving group X, aromatic ring Ar, heterocyclo ring-pyridine, heteroatom substrate E and the phosphine ligands.

COMPUTATIONAL METHODS

In order to choose a suitable level of theory for describing the structure and energetics of putative intermediates in these reactions, calculation of the geometries of important intermediates (e.g. **1**, **2** and **3** in Fig. 2) were performed at different levels of theory—restricted Hartree Fock (RHF), Møller–Plesset second-order perturbation theory (MP2) and several different density functional theories (DFTs). Comparison with x-ray structural data for experimental models indicates the unsuitability of RHF for this task, whereas both MP2 and all the DFTs tested (local and non-local) seem to predict geometries with acceptable accuracy ($\sim$ 2% difference maximum, and average differences of 1%).

For the basic oxidative addition and reductive elimination processes that comprise the catalytic cycle, MP2 and DFT provide comparable calculated reaction energies. Because no experimental data are available, the comparison is made by the calculation of energetics with coupled cluster (CCSD(T)) wavefunctions, a methodology that has been shown to reproduce experimental energies to within a few kcal mol^{-1}.[15] It is found that the calculated reaction energetics are comparable for the B3LYP DFT and the CCSD(T) level of theory using the same basis sets.

The Stevens effective core potential/valence basis scheme,[16] augmented with polarization functions on main group elements, which we have termed SBK(d), and validated in previous research, is utilized for calculations. The reactants, intermediates, transition states and products discussed in this paper are geometry optimized and vibrational frequencies are calculated using the Becke three-parameter hybrid B3LYP DFT.[17] All calculations are performed using Gaussian 98 software.[18]

The polarized continuum model (PCM)[19] was employed to model solvent effects. Standard parameters for toluene were employed.

Unless stated otherwise, quoted energetics are B3LYP/SBK(d) Gibbs free energies (298.15 K and 1 atm) determined at geometries optimized using this same level of theory. The energies include zero point energy and enthalpic and entropic corrections determined using B3LYP/SBK(d) vibrational frequencies, without scaling.

RESULTS AND DISCUSSION

The catalytic cycle with Pd–monophosphine complexes

For potential energy surface scans using the B3LYP/SBK(d) approach, a simplified model is investigated. In Eqn (2) $Pd(PH_3)_n$ is the simplified model for catalyst $Pd(PR_2(Ar–Ar'))_n$, whereas NH_3 is used to represent the heteroatom substrate. In the initial series of calculations a monophosphine Pd complex ($n = 1$) is the active catalytic species. A diphosphine Pd catalyst ($n = 2$) will be discussed later.

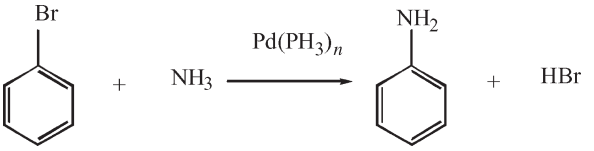

(2)

Oxidative Addition of Ph–Br. Oxidative addition of Ph–Br to $Pd(PH_3)$ yields the three-coordinate, 14-electron species $Pd(PH_3)(Ph)(Br)$. The initial interaction between the substrate PhBr and the catalyst $Pd(PH_3)$ shows that $(H_3P)Pd$—Br-Ph (**A1**, Fig. 3) bonds through the π ring of PhBr to the Pd with a binding free energy of -10.8 kcal mol^{-1}. Not surprisingly, π complexes are energetically preferred to Pd—Br σ complexes. Interestingly, the geometries of the π minima suggest a preference for η^1 instead of η^2 or η^6 coordination modes for the Pd–π interaction, for reasons that are not clear to us. The aryl–bromide oxidative addition product, $Pd(PH_3)(Ph)(Br)$, has three T-shaped isomers, with the *trans* position to open-coordination site being occupied by PH_3 (**1a**), Br (**1b**) or Ph (**1c**), as shown in Fig. 3. Aryl bromide **1c** is most stable (3 and 8 kcal mol^{-1} lower in energy than **1a** and **1b**, respectively), a result consistent with Ph being more strongly *trans*-influencing than PH_3 and Br. The calculated free energy for the reaction (from separated reactants) $Pd(PH_3) + Ph\text{-}Br \rightarrow$ **1c** is -15.4 kcal mol^{-1}.

Two possible transition states for oxidative addition of Ph–Br to $Pd(PH_3)$ are found, one with Ph *trans* to PH_3 (**T1b**‡) and, the other with Br *trans* to PH_3 (**T1c**‡) (Fig. 3). Thus, there are two possible reaction paths: $Pd(PH_3) +$ Ph–Br $\rightarrow$ **T1b**$^{\ddagger} \rightarrow$ **1b** or $Pd(PH_3) +$ Ph–Br $\rightarrow$ **T1c**$^{\ddagger} \rightarrow$ **1c**. Isomer **1a** can be generated from the isomerization of **1b** or **1c**, although not directly from oxidative addition of PhBr to Pd–phosphine. The calculations indicate little kinetic discrimination between the two oxidative addition transition states; **T1b**‡ is only 1.3 kcal mol^{-1} lower in energy than **T1c**‡. On the other hand, there is a more pronounced thermodynamic preference for **1c**, which is 7.9 kcal mol^{-1} more stable than **1b**.

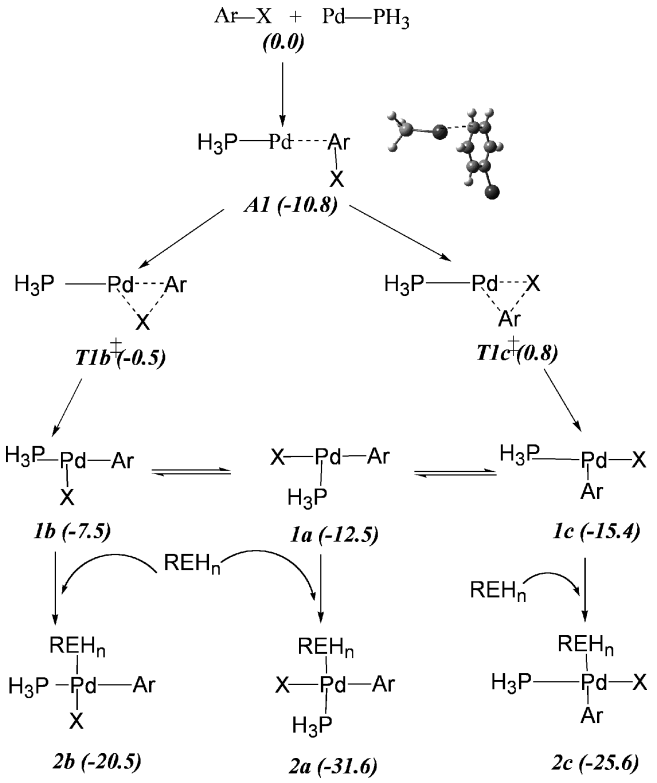

Figure 3. Oxidative addition and coordination steps. The numbers in parentheses are the Gibbs free energies relative to that of reactants (kcal mol^{-1}), which are PhBr, NH_3 and $Pd(PH_3)$ (X = Br, Ar = Ph, $REH_n = NH_3$)

Coordination of the heteroatom substrate NH_3. Substrate coordination is a straightforward process (Fig. 3) for the small models employed here. The ammine coordination product has three isomers (**2a, 2b** or **2c**) produced by coordination of ammonia from the three isomers (**1a, 1b** or **1c**) formed in the PhBr oxidation addition. Ammine **2a** of $Pd(PH_3)(NH_3)(Ph)(Br)$, NH_3 and PH_3 is *trans*, predicted by theory to be the lowest in energy by 6 kcal mol^{-1}. However, note that **2a** is formed from coordination of ammonia to **1a**, the oxidative addition product for which there is no direct path-to-from reactants. Hence, substantial formation of ammine **2a** would require isomerization of **1c** and/or **1b** to **1a** before heteroatom substrate coordination. Calculations indicate that the isomerization pathway from **1c** to **1a** is kinetically feasible with a barrier of $\sim$4.6 kcal mol^{-1}.

Elimination of HBr. Upon coordination of the heteroatom substrate, an equivalent of HX (in this case HBr) must be lost to yield $Pd(PH_3)(NH_2)(Ph)$, from which the aniline product is formed and the catalyst regenerated. The loss of HX can occur in one or two steps. In a single-step process, which is rare for middle to late transition metal complexes,[20] 1,2-HBr elimination shows a very high endothermicity (48 kcal mol^{-1}). The calculation is based on the energy of ammine **2a** (the most stable isomer of $Pd(Br)(PH_3)(NH_3)(Ph)$) and amide **3c** (the most stable isomer of $Pd(PH_3)(NH_2)(Ph)$; see next section).

It has been proposed that the role of external bases such as *t*-butoxide is to deprotonate the heteroatom substrate upon its coordination to the metal.[6,7] This suggests that 1,2-HX elimination may occur in two steps: proton abstraction by an external base (*t*-butoxide was used in this study) followed by liberation of bromide:

$$Pd(Br)(PH_3)(NH_3)(Ph) + tBuO^- \rightarrow [Pd(Br)(PH_3)(NH_2)(Ph)]^- + {}^tBuOH \quad (3a)$$

2a

$$[Pd(Br)(PH_3)(NH_2)(Ph)]^- \rightarrow [Pd(PH_3)(NH_2)(Ph)] + Br^- \quad (3b)$$

3c

Gas-phase calculation shows that the first step Eqn (3a) is exergonic by 28.3 kcal mol^{-1}, although the second step Eqn (3b) is endergonic by 19.4 kcal mol^{-1}. Because the energies of ions are greatly influenced by solvent, the most prevalent experimental solvent (toluene) is then modeled in the calculations. The PCM implemented in Gaussian 98 is used.[19] Upon inclusion of the solvent effects the first step is still highly exergonic (19.2 kcal mol^{-1}), but the second step is now only endergonic by 6.9 kcal mol^{-1}. Thus, our calculations suggest that HX elimination is a two-step process.

Reductive elimination. Research by Hartwig suggests that two pathways are possible in palladium-catalyzed amination.[7] Reductive elimination of product can happen from either mono- or diphosphine complexes: $Pd(PH_3)_n(NH_2)(Ph)$, where $n = 1$ or 2.

For a monophosphine active species, two $Pd(PH_3)(NH_2)Ph$ complexes are found as shown in Fig. 4: amide **3b** (NH_2 *trans* to open site) and amide **3c** (Ph *trans* to open site). Surprisingly, when geometry optimization starts from amide **3a** (PH_3 *trans* to open site), it converges to the **3c** isomer. Thermodynamically, **3c** is more stable than **3b** by 9.1 kcal mol^{-1}. Two reductive elimination transition states are found: **T3b**‡, with Ph *trans* to PH_3, is the transition state for **3b** $\rightarrow PdPH_3 + PhNH_2$, transition state **T3c**‡, with NH_2 *trans* to PH_3, is the transition state for the reaction **3c** $\rightarrow PdPH_3 + PhNH_2$ (Fig. 4). The kinetic barrier of the latter (11.8 kcal mol^{-1}) is 1.3 kcal mol^{-1} higher than the former (13.1 kcal mol^{-1}) (Fig. 4). Because **3c** is 9.1 kcal mol^{-1} more stable than **3b**, we conclude that the reductive elimination pathway for a monophosphine catalyst model is **3c** $\rightarrow$ **T3c**‡ $\rightarrow PdPH_3 + PhNH_2$.

If the elimination starts from diphosphine, as shown in Fig. 4, two isomers are found, **4b** (*trans*) and **4c** (*cis*). *Cis*

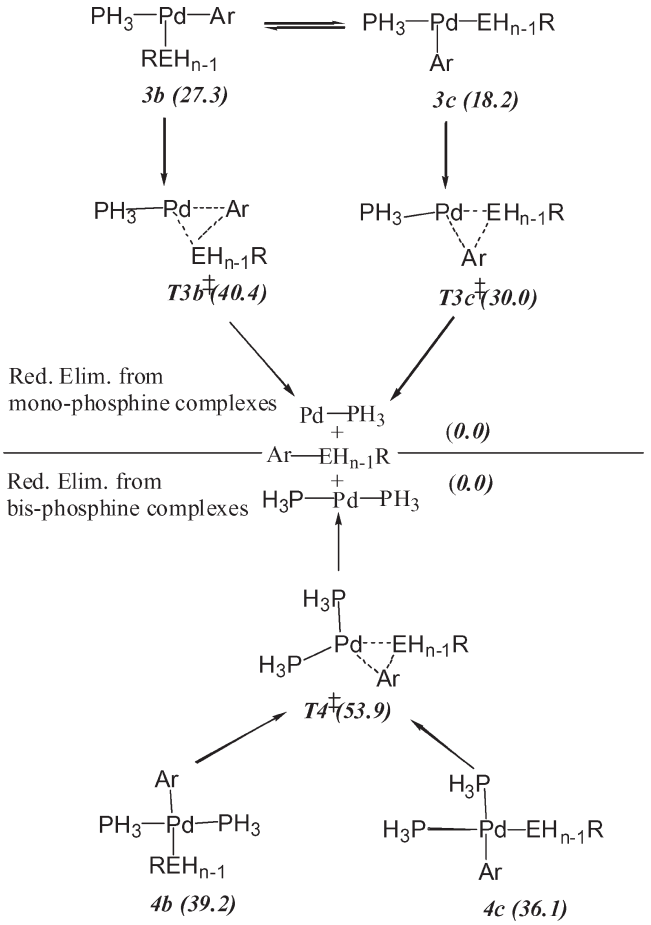

Figure 4. Reductive elimination. The numbers in parentheses are Gibbs free energies (kcal mol^{-1}) relative to those of $PhNH_2$ and $Pd(PH_3)/Pd(PH_3)_2$ (Ar = Ph and $REH_{n-1} = NH_2$)

isomer **4c** is more stable than *trans* **4b** by 3.1 kcal mol^{-1}. Even though the reaction from **4c** to $PhNH_2$ is 36 kcal mol^{-1} exergonic, the reductive elimination barrier from **4c** to transition state **T4**‡ is high at 17.8 kcal mol^{-1} (the barrier starting from monophosphine is 11.7 kcal mol^{-1}). In addition, the calculated energy for the hypothetical reaction **T4**‡ → **T3c**‡ + PH_3 is −5.1 kcal mol^{-1}. Thus, reductive elimination from diphosphine appears to be disfavored in relation to that for monophosphine.

β-H Elimination (NH_3 vs. NH_2CH_3)

β-H Elimination is a side-reaction that competes with reductive elimination (Fig. 5). The NH_2CH_3 substrate is studied instead of NH_3 in order to compare the kinetics and thermodynamics of β-H elimination with reductive elimination. Of course, introducing NH_2CH_3 does not change the Ar–Br oxidation addition process. Likewise, NH_3 and NH_2CH_3 also follow nearly identical paths with respect to coordination to Pd, elimination of HBr and elimination of Ph–amine (Fig. 5).

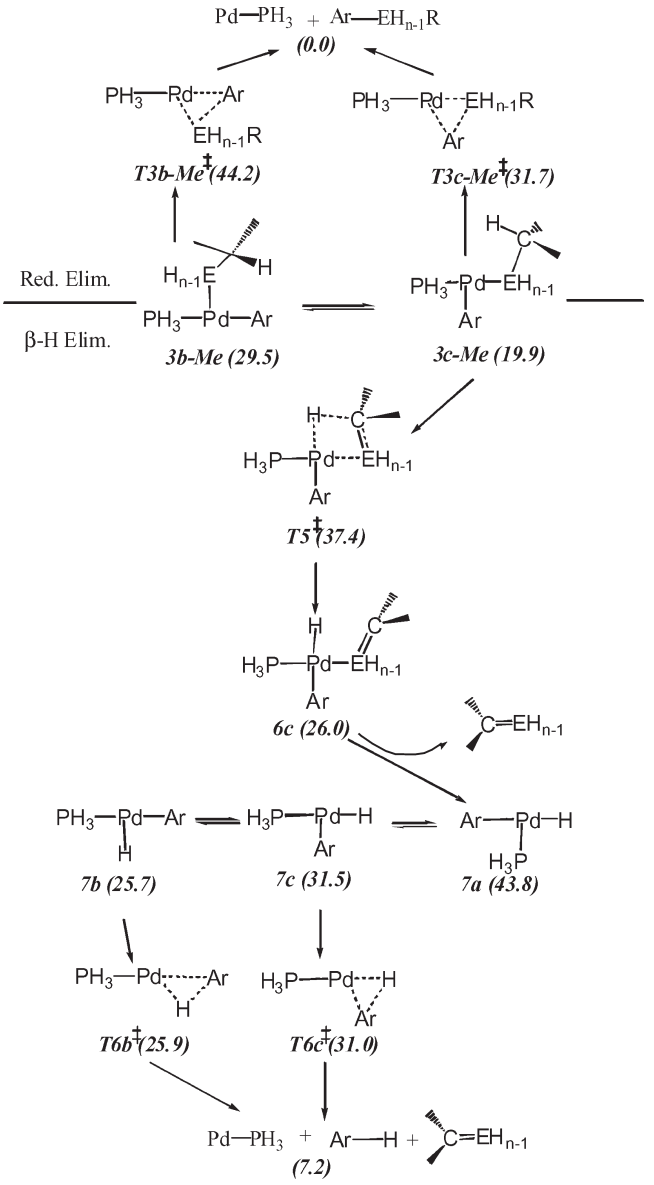

Figure 5. Reductive elimination and β-H elimination. The numbers in parentheses are the Gibbs free energies (kcal mol^{-1}) relative to those of $Ph(NHCH_3)$ and $Pd(PH_3)$ (Ar = Ph and $EH_{n-1}R = NHCH_3$)

Hydrogens on the methyl group may initiate the side-reaction of β-H elimination, which competes with $Ph(N(H)CH_3)$ reductive elimination. The β-H elimination process starts from amide **3c-Me** (the lower energy conformation), goes through transition state **T5**‡ and forms the four-coordination intermediate **6c**. By liberating imine ($HN{=}CH_2$), intermediate **6c** produces $Pd(Ph)(PH_3)(H)$ with three T-shaped isomers, the *trans* position to the open coordination site being occupied by PH_3 (**7a**), H (**7b**) and Ar (**7c**) (Fig. 5). Because H and Ar groups have much stronger *trans*-influencing effects than PH_3 group, **7b** and **7c** are both lower than **7a** in energy. Isomer **7b** is favored by 5.7 kcal mol^{-1} versus **7c**. Isomers **7b** and **7c** can go through transition states **T6b**‡ and **T6c**‡,

respectively, and both passes lead to the side-product arene (in our case, benzene). This step is very facile because the barrier is <1 kcal mol^{-1} (Fig. 5).

Thus, the β-H elimination side–reaction includes one major barrier: **3c-Me** $\rightarrow$ **T5**‡ (17.5 kcal mol^{-1}). On the other hand, the kinetic barrier for the reductive elimination step **3c-Me** $\rightarrow$ **T3c-Me**‡ is 12 kcal mol^{-1}. The energetics for the side-reaction and reductive elimination are -12.7 and -20.0 kcal mol^{-1}, respectively. This shows that β-H elimination is less favored than the reductive elimination from both thermodynamic and kinetic viewpoints.

Active catalytic species ($Pd(PH_3)$ vs. $Pd(PH_3)_2$)

Until now, we have assumed a monophosphine active species based on experimental evidence.[9] In order to address computationally the active catalytic species (monophosphine versus diphosphine Pd complexes), two issues need to be addressed: the relative kinetic barrier of the oxidation addition of ArX and the stability of $Pd(PH_3)$ versus $Pd(PH_3)_2$.

If the active catalytic species is a diphosphine complex, the oxidative addition step will be different. As shown in Fig. 6, reactant PhBr and catalyst $Pd(PH_3)_2$ first

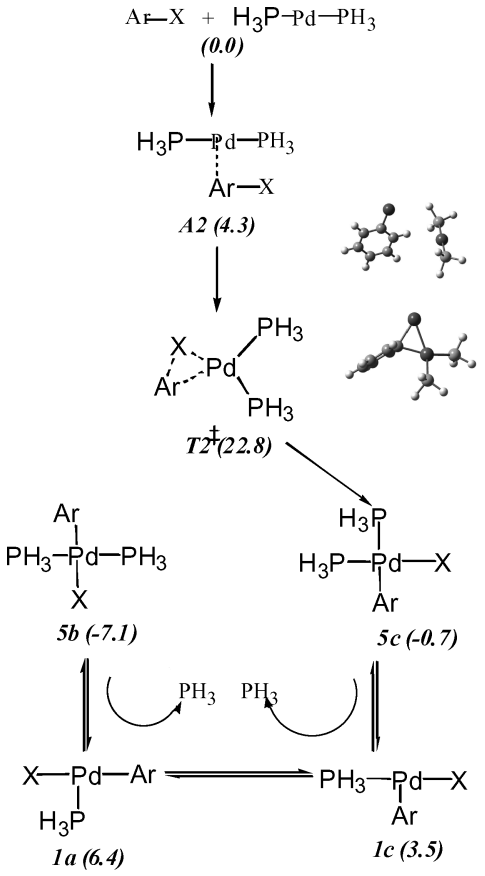

Figure 6. Oxidative addition of Ph–Br to $Pd(PH_3)_2$. The numbers in parentheses are the Gibbs free energies (kcal mol^{-1}) relative to those of PhBr and $Pd(PH_3)_2$

form adduct **A2**, which is essentially unbound ($\Delta G = 4.3$ kcal mol^{-1}) upon inclusion of entropic corrections. Adduct **A2** then proceeds to transition state **T2**‡ and produces **5c**, *cis*–$Pd(PH_3)_2(Br)(Ph)$. *Trans* isomer **5b** is more stable than *cis* **5c** by 6.4 kcal mol^{-1}. The isomerization between **5c** and **5b** involves three-coordinated species **1c** and **1b** after losing one phosphine ligand from four-coordinated diphosphine-ligand species. Even though the overall oxidative addition is 7.1 kcal mol^{-1} exergonic, the kinetic barrier from **A2** to transition state **T2**‡ is 18.5 kcal mol^{-1}, which is 8 kcal mol^{-1} higher than that of monophosphine oxidative addition. In addition, the calculated ΔG for the hypothetical reaction **T2**$^{\ddagger} \rightarrow$ **T1b**$^{\ddagger} + PH_3$ is -4.3 kcal mol^{-1}, which further supports the energetic preference for a monophosphine active species.

Direct coordination of NH_3 to form a five-coordinate intermediate from **5b** is not favored. All attempts at geometry optimization to identify a stable $Pd(NH_3)(PH_3)_2(Ph)Br$ resulted in loss of ammonia. However, the process of exchanging PH_3 with NH_3 (**5b** $+ NH_3 \rightarrow$ **2a** $+ PH_3$) is 5.6 kcal mol^{-1} exergonic.

Reductive elimination to form an aniline product from the diphosphine Pd complexes is disfavored relative to the analogous process for monophosphines discussed earlier.

Experimental evidence, particularly NMR spectroscopy, has been interpreted to indicate that the active species for the most active catalysts are Pd–monophosphine complexes $Pd[PR_2(Ar–Ar')]$, where R is typically a bulky alkyl group, such as cyclohexyl (Cy) or *t*-butyl (^{t}Bu), and Ar–Ar$'$ is a biphenyl derivative.[9] However, phosphine dissociation from $Pd(PH_3)_2$ to $Pd(PH_3)$ is 19 kcal mol^{-1} exergonic. Because our simplified system ignores the steric effect of the phosphine ligand, the energetics for phosphine dissociation need to be justified using more realistic models. This is currently being explored in our laboratory by hybrid quantum mechanics and molecular mechanics (QM/MM) techniques. Our preliminary results suggest that monophosphines are stabilized by Pd–π interactions with the pendant Ar$'$ group, hence all the preceding and ensuing discussion is based on a Pd–monophosphine active species.

The effect of different X groups (Cl vs. Br)

In experiment, the use of aryl chlorides rather than bromides or iodides in cross-coupling chemistry has been actively pursued because of the low cost of the former.[21] In our calculations, they follow very similar reaction paths. The lowest energy isomers for the different reaction intermediates ($Pd(PH_3)(Ph)X$ and $Pd(PH_3)(Ph)(NH_3)X$) are also similar in geometry for X = Cl and X = Br. The overall free energy for oxidative addition from separated reactants is -11.3 kcal mol^{-1} for PhCl versus -15.4 kcal mol^{-1} for PhBr. Furthermore, the barrier from adduct to transition state is 18.3 kcal mol^{-1}

for chlorobenzene versus 10.4 kcal mol^{-1} for bromobenzene (Table 1). The lower barrier for oxidative addition of the aryl bromide is consistent with the mechanistic data of Buchwald and co-workers.[6] Substitution of Br with Cl also disfavors the coordination of amine by 3 kcal mol^{-1}.

The 1,2-HX elimination process (gas phase) favors HCl elimination (43.5 kcal mol^{-1}) versus HBr elimination (48.0 kcal mol^{-1}) by 4.5 kcal mol^{-1}. However, calculation of the two-step elimination with toluene solvent (see Eqns (3a) and (3b)) shows that liberation of chloride is 12.0 kcal mol^{-1} endergonic, which is 5.1 kcal mol^{-1} higher than that of bromide (6.9 kcal mol^{-1}) (Table 1). Thus, aryl chlorides hinder the overall reaction by increasing the barrier to oxidative addition as well as HCl elimination.

The effect of Ar group (PhBr vs. ArBr)

The role of electronic effects in modifying the reaction is investigated by comparison of the computed kinetics and thermodynamics of bromobenzene with that of *p*-substituted aryl bromides such as *p*-NH_2–C_6H_4Br (electron rich) and *p*-CN–C_6H_4Br (electron poor).

The calculation of the energetics for the overall reaction ($Ar–Br + NH_3 \rightarrow HBr + Ar–NH_2$) indicates that *p*-$NH_2$–$C_6H_4Br$ disfavors the reaction by 2.9 kcal mol^{-1} ($\Delta G = 1.0$ kcal mol^{-1}) and *p*–CN–C_6H_4Br favors the reaction by 2.9 kcal mol^{-1} ($\Delta G = -4.8$ kcal mol^{-1}) compared with C_6H_5Br (Table 1). The electron-withdrawing *p*-cyano group yields lower oxidative addition (by 3.9 kcal mol^{-1}) and reductive elimination (by 0.5 kcal mol^{-1}) barriers versus bromobenzene. On the other hand, amino substitution lowers the oxidative addition barrier by 1.0 kcal mol^{-1}, but raises the reductive elimination barrier by 0.4 kcal mol^{-1} versus bromobenzene. Experimentally, acceleration of C—N[22] and C—O[23] bond formation was observed with complexes containing aryl groups with electron-withdrawing substituents, a result consistent with the present computations if one assumes that the rate-determining step is either oxidative addition of ArX or reductive elimination of the product.

The effect of heterocycle (PyBr vs. PhBr)

Because the pyridine moiety exists in many synthetic drugs, fungicides and herbicides (i.e. epibatidine and nicotine in Fig. 7), it would be of interest to know the effect when the bromopyridine replaces aryl bromide as substrate. We focused on 2-bromopyridine and 3-bromopyridine, which are more of experimental interest.[9] Theoretically, due to the electronegativity of the nitrogen atom, the 2nd and 4th positions bear a partial positive charge, making them prone to nucleophilic attack by the catalyst during the oxidative addition step. Experimentally, aminations of 2-chloropyridine were observed to be considerably faster than those of 3-chloropyridine.[6]

Table 1. Summary of reaction energetics (Gibbs free energy, kcal mol^{-1}) with different reactants or catalysts

Reactant $ArX + REH_n$	Catalyst PL_n	Oxidative addition[a] $ArX + PdL_n \rightarrow PdL_n(Ar)(X)$	Coordination $\rightarrow PdL_n(Ar)(X)(REH_n)$	HX Elimination[b] $\rightarrow PdL_n(Ar)(REH_{n-1})$	Reductive elimination[a] $\rightarrow ArEH_{n-1}R + PdL_n$	Overall reaction $ArX + REH_n \rightarrow ArEH_{n-1} + HX$
$PhBr + NH_3$	$Pd(PH_3)$	−15.4 (10.4)	−19.1	48.0 (−19.2, 6.9)	−18.2 (11.7)	−1.9
$PhBr + NH_2(CH_3)$	$Pd(PH_3)$	−15.4 (10.4)	−18.0	46.7 (−14.7, 1.2)	−19.9 (11.8)	−3.7
$PhBr + NH_3$	$Pd(PH_3)_2$	−7.1 (18.5)	−5.6	48.0 (−19.2, 6.9)	−36.1 (17.8)	−1.9
$PhCl + NH_3$	$Pd(PH_3)$	−11.3 (18.3)	−15.7	43.5 (−19.1, 12.0)	−18.2 (11.7)	−1.7
$PhBr(p\text{-}NH_2) + NH_3$	$Pd(PH_3)$	−14.7 (9.4)	−14.7	47.2 (−19.7, 6.7)	−16.7(12.1)	1.0
$PhBr(p\text{-}CN) + NH_3$	$Pd(PH_3)$	−15.7 (6.5)	−16.1	46.3 (−27.6, 13.7)	−19.3 (11.2)	−4.8
$2\text{-}PyBr + NH_3$	$Pd(PH_3)$	− 19.3 (9.0)	−12.4	46.6 (−19.7, 6.1)	− 21.6 (10.3)	−6.8
$3\text{-}PyBr + NH_3$	$Pd(PH_3)$	− 12.7 (12.0)	−19.5	47.2 (−23.9, 10.9)	− 17.5 (12.3)	−2.4
$PhBr + H_2O$	$Pd(PH_3)$	−15.4 (10.4)	−7.5	34.9 (−37.2, 11.9)	−16.7 (15.8)	−1.8
$PhBr + NH_3$	$Pd[P(CH_3)_3]$	−20.7 (9.3)	−15.1	50.7 (−7.3, −2.2)	−16.8 (12.9)	−1.9

[a] Numbers in parentheses correspond to the kinetic barrier.
[b] The first value corresponds to the Gibbs free energy in the one-step HX elimination in the gas phase. The values in parentheses correspond to the two-step HX elimination in toluene: abstraction of photon and the liberation of halide.

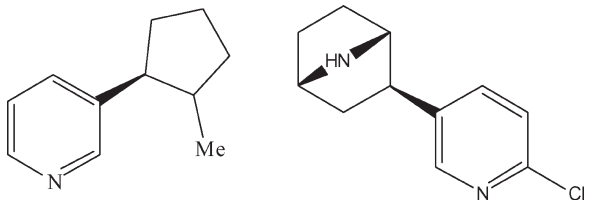

Figure 7. Structures of epibatidine (left) and nicotine (right)

In our calculation, 2-Br–Py yields lower barriers (both by 1.4 kcal mol^{-1}) of oxidative addition and reductive elimination compared with those of Ph–Br. On the other hand, 3-Br–Py increases oxidative addition (by 1.6 kcal mol^{-1}), reductive elimination (by 0.6 kcal mol^{-1}) and HBr loss (by 4 kcal mol^{-1}) barriers relative to bromobenzene. Thus, the greater activity of 2-Br–Py than 3-Br–Py is not only caused by the difference in the oxidative addition step but also HX loss and reductive elimination steps.

The effect of different E groups (NH_3 vs. H_2O)

Substitution of NH_3 with H_2O will permit an examination of the catalytic process of producing aryl ethers, which remains a major challenge for organic synthesis.[6–8] The observed differences in catalytic aryl–O and aryl–N formation for otherwise similar catalyst systems[6,7] are investigated by comparison of the relative kinetics and thermodynamics for H_2O versus NH_3 coordination and reductive elimination to form C—O versus C—N bonds, respectively.

Coordination of H_2O to $Pd(PH_3)(Ph)Br$ is still exergonic ($\Delta G = -7.5$ kcal mol^{-1}) even though it is 11.6 kcal mol^{-1} less favorable than coordination of NH_3 (Table 1). Thus, it does not seem as if the differences in aryl ether versus aryl amine synthesis are due to some inherent unfavorability of substrate coordination for oxygen-containing heteroatom substrates.

The 1,2-HBr elimination process (gas phase) seems to be easier from $Pd(PH_3)(H_2O)(Ph)(Br)$ ($\Delta G_{rxn} =$ 34.9 kcal mol^{-1}) than $Pd(PH_3)(NH_3)(Ph)(Br)$ ($\Delta G_{rxn} =$ 48.0 kcal mol^{-1}) by 13.1 kcal mol^{-1}. However, calculation of two-step HX elimination (toluene solvent) shows that for the aqua complex the deprotonation step is -37.2 kcal mol^{-1} (-19.2 kcal mol^{-1} for the ammine) and liberation of bromide is 11.9 kcal mol^{-1} (6.9 kcal mol^{-1} for the ammine) (Table 1). Thus, substitution of NH_3 with H_2O retards HBr elimination by increasing the energy of bromide loss.

For the reductive elimination step, only one transition state is found, that in which the OH group is *trans* to phosphine (**T3c**‡ in Fig. 4). The reductive elimination barrier for C_{aryl}—O bond formation is 15.8 kcal mol^{-1} to produce phenol, which is 3 kcal mol^{-1} higher than the barrier to C_{aryl}—N formation to produce aniline. Thus, the differences in reactivity for aryl ether versus aryl amine products thus seems to be due to the higher reductive elimination barrier for the former, although the effect of the E-containing substrate on HX loss cannot be discounted.

The effect of phosphine ligand modification (PMe_3 vs. PH_3)

The phosphine ligands in the experimental systems require electron-rich as well as sterically bulky substituents,[6] whereas the model PH_3 has neither of these properties. The replacement of PH_3 with PMe_3 was investigated to provide an assessment of how a larger and more electron-donating phosphine may affect the catalytic cycle.

Differences are found upon going from a $Pd(PH_3)$ to a $Pd(PMe_3)$ catalyst model. First, among the three Ph–Br oxidative addition isomers (**1a**, **1b** and **1c**), **1a** is slightly more stable than **1c** by 0.6 kcal mol^{-1} for the PMe_3-substituted system in contrast to the $Pd(PH_3)$ system (**1a** < **1c** by 2.9 kcal mol^{-1}). Second, 1,2-HBr elimination is even more disfavored in the gas phase (51 kcal mol^{-1} for PMe_3 versus 48 kcal mol^{-1} for PH_3). However, if toluene solvent effects are considered for the two-step HBr elimination (see Eqns (3a) and (3b)) then both steps are exergonic: the deprotonation by *t*-butoxide is -7.3 kcal mol^{-1} (-19.2 kcal mol^{-1} for the PH_3 system) and bromide loss is -2.2 kcal mol^{-1} (6.9 kcal mol^{-1} for the PH_3 system). Third, the PMe_3 ligand facilitates oxidative addition (the barrier is 1.1 kcal mol^{-1} lower for PMe_3 versus the PH_3 catalyst model) and hinders reductive elimination (the barrier is 1.2 kcal mol^{-1} higher) (Table 1) which is consistent with PMe_3 being a better donor than PH_3.

SUMMARY

A DFT study of the kinetics and thermodynamics of Pd–phosphine–catalyzed heteroatom bond formation (Eqn (1)) was carried out. Individual steps in the catalytic cycle—ArX oxidative addition, REH_n coordination, HX loss, $ArE(H)_{n-1}R$ reductive elimination and β-H elimination—were investigated. The effects of modification of the ligand (PH_3 versus PMe_3), leaving group (X = Cl versus X = Br), heteroatom substrate ($REH_n = H_2O$ and NH_3), aryl (Ar = phenyl, *p*-cyanophenyl, *p*-aminophenyl and pyridyl) and metal coordination number ($Pd(PH_3)$ versus $Pd(PH_3)_2$), were investigated. Major conclusions are summarized here:

(i) Aryl chlorides hinder the overall amination reaction by increasing the barrier to the initial oxidative addition relative to aryl bromides. Also, HX loss is more favorable for X = Br than X = Cl.
(ii) *Para* electron-withdrawing groups on the aryl ring facilitate both the oxidative addition and reductive elimination steps.

(iii) 2-Halopyridines are more active than 3-halopyridines by facilitating oxidative addition, HX loss and reductive elimination.
(iv) More weakly coordinated heteroatom substrates (i.e. alcohol versus amine) will hinder the reaction by increasing the reductive elimination barrier and increasing the barrier to bromide loss.
(v) Electron-rich phosphine ligands facilitate the oxidative addition step and hinder reductive elimination.
(vi) The exact nature of the catalyst active species is predicted to be a monophosphine Pd complex because it allows lower oxidative addition and reductive elimination barriers than diphosphine Pd complexes. However, more realistic models are needed to model the steric effect of the phosphine ligands on the active catalytic species.

Acknowledgments

The authors acknowledge the support of the National Science Foundation through grant CHE-9983665. This research was carried out while the authors were on the staff at the University of Memphis Department of Chemistry; the authors thank the Department for its support of this work. The authors acknowledge computing centers at the University of Kentucky and Advanced Biomedical Computing Center (National Cancer Institute) for allowing supercomputing time. J.D. also wants to thank the fellowships offered by the University of Memphis Society and Women's Research Forum.

Supplementary material

Cartesian coordinates (in A) for stationary points in this research (31 pages) are available in Wiley Interscience.

REFERENCES

1. Hegedus LS. *Transition Metals in the Synthesis of Complex Organic Molecules* (2nd edn). University Science Books: Sausalito, 1999.
2. Trost BM, Van Vranken DL. *Chem. Rev.* 1996; **96**: 395–422; Trost BM. *Pure Appl. Chem.* 1996; **68**: 779–784; Tsuji J. *Pure Appl. Chem.* 1999; **71**: 1539–1547; Malleron JL, Fiaud JC, Legros JY. *Handbook of Palladium-catalyzed Organic Reactions*. Academic Press: San Diego, 1997.
3. Amatore C, Jutand C, Suzuki A. *J. Organomet. Chem.* 1999; **576**: 254–278; Crisp GT. *Chem. Soc. Rev.* 1998; **27**: 427–436; Amatore C, Jutand A. *Acc. Chem. Res.* 2000; **33**: 314–321; Beletskaya IP, Cheprakov AV. *Chem. Rev.* 2000; **100**: 3009–3066.
4. Stille JK. *Angew. Chem., Int. Ed. Engl.* 1986; **25**: 508–523; Maleczka RE, Gallagher WP, Terstiege I. *J. Am. Chem. Soc.* 2000; **122**: 384–385.
5. Miyaura N, Suzuki A. *Chem. Rev.* 1995; **95**: 2457–2483; Suzuki A. *J. Organomet. Chem.* 1999; **576**: 147–168; Buchwald SL, Fox JM. *Strem Chem.* 2000; **XVIII**: 1–12.
6. Yang BH, Buchwald SL. *J. Organomet. Chem.* 1999; **576**: 125–146; Wolfe JP, Wagaw S, Marcoux JF, Buchwald SL. *Acc. Chem. Res.* 1998; **31**: 805–818; Wolfe JP, Tomori H, Sadighi JP, Yin J, Buchwald SL. *J. Org. Chem.* 2000; **65**: 1158–1174.
7. Hartwig JF. *Acc. Chem. Res.* 1998; **31**: 852–860; Hartwig JF. *Angew. Chem., Int. Ed. Engl.* 1998; **37**: 2046–2067; Mann G, Incarvito C, Rheingold AL, Hartwig JF. *J. Am. Chem. Soc.* 1999; **121**: 3224–3225; Alcazar-Roman LM, Hartwig JF, Rheingold AL, Liable-Sands LM, Guzei IA. *J. Am. Chem. Soc.* 2000; **122**: 4618–4630.
8. Fagan PJ, Hauptman E, Shapiro R, Casalnuvo A. *J. Am. Chem. Soc.* 2000; **122**: 5043–5051; Kalinin AV, Bower JF, Riebel P, Snieckus V. *J. Org. Chem.* 1999; **64**: 2986–2987; Zhang S, Zhang D, Liebeskind LS. *J. Org. Chem.* 1997; **62**: 2312–2313; Meyers AI, Willemsen JJ. *Chem. Comm.* 1997; 1573–1574; Price A, Meyers AI. *J. Org. Chem.* 1998; **63**: 412–413.
9. Walker SD, Barder TE, Martinelli JR, Buchwald SL. *Angew. Chem. Int. Ed. Engl.* 2004; **43**: 1871–1876.
10. Musaev DG, Mebel AM, Morokuma K. *J. Am. Chem. Soc.* 1994; **116**: 10693–10702; Musaev DG, Matsubara T, Mebel AM, Koga N, Morokuma K. *Pure Appl. Chem.* 1995; **67**: 257–263; Dorigo AE, Schleyer PvR. *Angew. Chem., Int. Ed. Engl.* 1995; **34**: 115–118; Cui Q, Musaev DG, Morokuma K. *Organometallics* 1997; **16**: 1355–1364; Sakaki S, Kikuno T. *Inorg. Chem.* 1997; **36**: 226–229.
11. Albert K, Gisdakis P, Rösch N. *Organometallics* 1998; **17**: 1608–1616; Hii KK, Claridge TDW, Brown JM, Smith A, Deeth RJ. *Helv. Chim. Acta* 2001; **84**: 3043–3056; Davies IW, Wu J, Marcoux JF, Taylor M, Hughes D, Reider P, Deeth RJ. *Tetrahedron* 2001; **57**: 5061–5066; Sundermann A, Uzan O, Martin JML. *Chem. Eur. J.* 2001; **7**: 1703–1711; Senn HM, Ziegler T. *Organometallics* 2004; **23**: 2980–2988; Lin BL, Liu L, Fu Y, Luo SW, Chen Q, Guo QX. *Organometallics* 2004; **23**: 2114–2123; McGuinness DS, Cavell KJ, Kingsley J, Yates BF, Skelton BW, White AH. *J. Am. Chem. Soc.* 2001; **123**: 8317–8328; Kozuch S, Shaik S, Jutand A, Amatore C. *Chem. Eur. J.* 2004; **10**: 3072–3080; Deeth RJ, Smith A, Brown JM. *J. Am. Chem. Soc.* 2004; **126**: 7144–7151; von Schenck H, Kermark B, Svensson M. *J. Am. Chem. Soc.* 2003; **125**: 3503–3508; Deeth RJ, Smith A, Hii KK, Brown JM. *Tetrahedron Lett.* 1998; **39**: 3229–3232.
12. Norrby PO, Mader MM, Vitale M, Prestat G, Poli G. *Organometallics* 2003; **22**: 1849–1855.
13. Kocovsky P, Vyskocil S, Cisarova I, Sejbal J, Tislerova I, Smrcina N, Lloyd-Jones GC, Stephen SC, Butts CP, Murray M, Langer V. *J. Am. Chem. Soc.* 1999; **121**: 7714–7715.
14. Tomori H, Fox JM, Buchwald SL. *J. Org. Chem.* 2000; **65**: 5334–5341.
15. Torrent M, Sola M, Frenking G. *Chem. Rev.* 2000; **100**: 439–494; Bartlett RJ, Stanton JF. *Rev. Comput. Chem.* 1994; **5**: 65–169.
16. Cundari TR, Gordon MS. *Coord. Chem. Rev.* 1996; **147**: 87–115; Benson MT, Cundari TR, Lutz ML, Sommerer SO. *Rev. Comput. Chem.* 1996; **8**: 145–202; Cundari TR. *Chem. Rev.* 2000; **100**: 807–818.
17. Becke AD. *J. Chem. Phys.* 1993; **98**: 5648–5652; Lee C, Yang W, Parr RG. *Phys. Rev. B* 1988; **37**: 785–789; Vosko SH, Wilk L, Nusair M. *Can. J. Phys.* 1980; **58**: 1200–1211.
18. Frisch MJ, Trucks GW, Schlegel HB, Scuseria GE, Robb MA, Cheeseman JR, Zakrzewski VG, Montgomery JA, Sratmann RE, Burant JC, Dapprich S, Millam JM, Daniels AD, Kudin KN, Strain MC, Farkas O, Tomasi J, Barone V, Cossi M, Cammi R, Mennucci B, Pomelli C, Adamo C, Clifford S, Ochterski J, Petersson GA, Ayala PY, Cui Q, Morokuma K, Malick DK, Rabuck AD, Raghavachari K, Foresman JB, Cioslowski J, Ortiz JV, Stefanov BB, Liu G, Liashenko A, Piskorz P, Komaromi I, Gomperts R, Martin RL, Fox DJ, Keith T, Al-Laham MA, Peng CY, Nanayakkara A, Gonzalez C, Challacombe M, Gill PMW, Johnson B, Chen W, Wong MW, Andres JL, Gonzalez C, Head-Gordon M, Replogle ES, Pople JA. *Gaussian 98, Revision A.9*. Gaussian, Inc.: Pittsburgh, PA, 1998.
19. Tomasi J, Persico M. *Chem. Rev.* 1994; **94**: 2027–2094.
20. Bryndza H, Tam W. *Chem. Rev.* 1988; **88**: 1163–1195.
21. Hartwig JF, Kawatsura M, Hauck SI, Shaughnessy KH, Alcazar-Roman LM. *J. Org. Chem.* 1999; **64**: 5575–5580.
22. Driver MS, Hartwig JF. *J. Am. Chem. Soc* 1997; **119**: 8232–8243.
23. Aranyos A, Old DW, Kiyomori A, Wolfe JP, Sadighi JP, Buchwald SL. *J. Am. Chem. Soc.* 1999; **121**: 4369–4378.